arXiv:1210.2386v1 [cond-mat.mes-hall] 8 Oct 2012

Valley Degenerate 2D Electrons in the Lowest Landau Level

Tomasz M. Kott,* Binhui Hu, S. H. Brown, and B. E. Kane
Laboratory for Physical Sciences & Joint Quantum Institute,
University of Maryland, College Park, MD 20740
(Dated: October 9, 2012)

We report low temperature magnetotransport measurements on a high mobility ($\mu = 325\,000\,\mathrm{cm^2/V\,sec}$) 2D electron system on a H-terminated Si(111) surface. While low magnetic field data indicate a six-fold valley degenerate system, we observe the integral quantum Hall effect at all filling factors $\nu \leq 6$ and find that $\nu = 2$ develops in an unusually narrow temperature range. An extended, exclusively even numerator, fractional quantum Hall hierarchy occurs surrounding $\nu = 3/2$, consistent with two-fold valley-degenerate composite fermions (CFs). We determine activation energies and estimate the CF mass.

PACS numbers: 73.40.-c, 73.43.-f, 71.70.Gm

Multicomponent systems in a single Landau level have generated interest due to the possibilities for novel correlated ground states in the integer and fractional quantum Hall (FQH) regimes when the energies of the component states become degenerate. Early experiments focused on measurements of engineered GaAs materials where the spin splitting could be reduced to zero [1, 2]. Subsequent development of AlAs quantum wells with a tunable valley degeneracy allowed the study of a spin-like degeneracy in the same limit [3]. Recently, there has been great interest in the sublattice (valley) degeneracy in graphene; experiments show that the valley symmetry affects the FQH hierarchy [4, 5] and that valley ferromagnetism occurs when one of two degenerate valleys is occupied [6].

Measurements on silicon, the first multi-valley system to be considered theoretically [8, 9], had been hampered by high disorder. Lately, however, Si(100)/SiGe heterostructures have shown mobilities up to $\sim 10^6\,\mathrm{cm^2/Vs}$ [10]. Nonetheless, Si(100) is known to have an intrinsic valley splitting due to surface effects [11–14]. The case of 2D electrons on (111) oriented silicon surfaces, which have three pairs of opposite momentum ($\vec{k}$) valleys, is especially interesting. As opposed to either AlAs or Si(100), valley pairs with $\pm\vec{k}$ symmetry in Si(111) cannot be broken within the effective mass approximation or by a surface potential [9], similar to the case of valleys in graphene. Additionally, both AlAs and Si(111) exhibit anisotropic mass tensors; in AlAs, this anisotropy arguably transfers to composite fermions [15]. Novel broken symmetry states have been predicted at integer filling factor, ν, when the Fermi energy, E_F, lies between two valleys with different mass tensors [16].

In this Letter we present transport data on a very high mobility electron system ($\mu = 325\,000\,\mathrm{cm^2/Vs}$ at a temperature $T = 90\,\mathrm{mK}$ and density $n_s = 4.15 \times 10^{11}\,\mathrm{cm^{-2}}$) on a hydrogen-terminated Si(111) surface. We discuss the anisotropy between orthogonal current directions and observe an extended FQH hierarchy around $\nu = 3/2$. We argue that the FQH hierarchy is consistent with the SU(2) symmetry of a valley-degenerate ground state, and estimate the mass of composite fermions. Finally, we present evidence for many-body interactions affecting activation energies of several integer filling factors. We find that the development of $\nu = 2$ occurs in an unusually narrow temperature range, and thus may signal a transition to broken symmetry valley states.

For our samples, we replace the Si-SiO$_2$ interface of a typical MOSFET with an interface between H terminated Si(111) and vacuum in order to remove the effects of strain and dangling bonds from the Si(111) surface [17]. This is done with the help of an encapsulating silicon-on-insulator piece which is bonded via van der Waals forces to a high resistivity H-Si(111) substrate and forms a gate. The sample studied in the present work is fabricated in the same way as previous ones, with further optimized cleaning and annealing steps [18]. Four-terminal resistance in a square van der Pauw geometry is defined as $R_{ij,lm} = V_{lm}/I_{ij}$, with $R_{xx} = R_{12,34}$ and $R_{yy} = R_{24,13}$ oriented along the $[1\bar{1}0]$ and $[11\bar{2}]$ directions respectively (see inset to Fig. 1b). Hall traces, ρ_{xy}, are the averages of $R_{14,23}$ and $R_{23,14}$ to prevent mixing. The data were obtained at densities between $n_s = 3.7$ and $5.7 \times 10^{11}\,\mathrm{cm^{-2}}$, adjustable via a gate voltage, in both a ^{3}He system and ^{3}He/^{4}He dilution system with base temperatures of 280 mK and 90 mK, respectively. The density range is limited due to nonlinear contact resistances at low n_s and gate leakage at high n_s. Magnetotransport measurements were performed using standard lock-in techniques with a typical excitation of $1 - 25\,\mathrm{nA}$ at 5 Hz in a magnetic field up to 12 T.

Figure 1a shows R_{xx}, R_{yy} and ρ_{xy} versus magnetic field B taken at $T = 90\,\mathrm{mK}$ and density $n_s = 3.75\times10^{11}\,\mathrm{cm^{-2}}$. Shubnikov-de Haas oscillations (SdHO) are visible down to about $B \sim 0.15\,\mathrm{T}$. At low B and before the onset of spin splitting, minima occur at $\Delta\nu_{xx} = 11.65 \pm 0.04$, while $\Delta\nu_{yy} = 12.6 \pm 0.1$, roughly consistent with a valley degeneracy $g_v = 6$ and a spin degeneracy $g_s = 2$. Due to the anisotropy between R_{xx} and R_{yy} (discussed below), we do not expect perfect agreement with $\Delta\nu = 12$. By $B \approx 1.3\,\mathrm{T}$ ($\nu = 12$), only the lowest Landau level

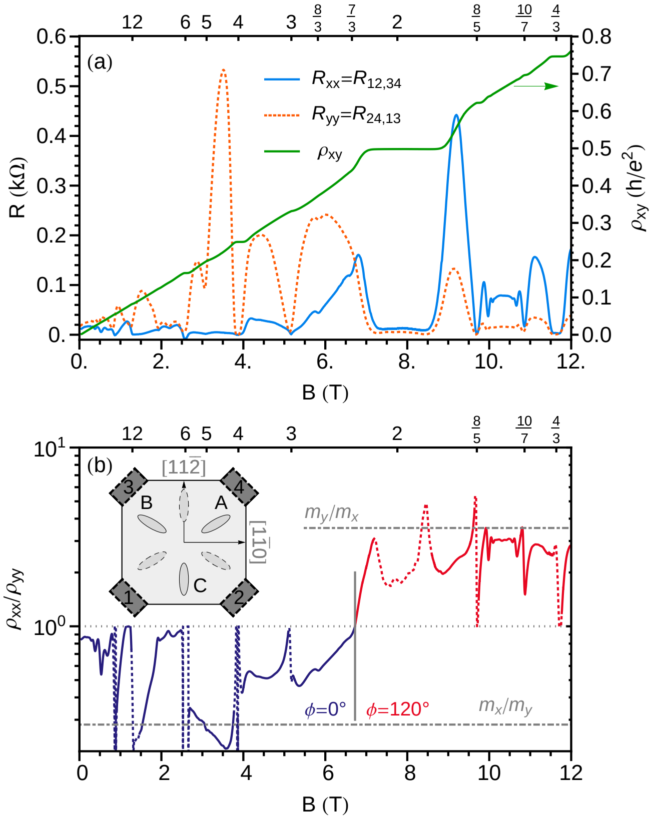

Figure 1. *(a)* R_{xx}, R_{yy} (left), and ρ_{xy} (right) vs. B at $T = 90\,\mathrm{mK}$ and $n_s = 3.75 \times 10^{11}\,\mathrm{cm}^{-2}$ with filling factors listed on the top axis; the fractional states at $\nu = \frac{8}{5}$, $\frac{10}{7}$, and $\frac{4}{3}$ have plateaus in ρ_{xy}. *(b)* Calculated anisotropy ρ_{xx}/ρ_{yy} for the same data as (a). Dotted lines indicate regions near filling factor minima, where R is small and leads to large errors. The dot-dashed lines show predicted anisotropy if only a single valley pair contributes to conduction (see inset and text). *Inset*: Schematic of the sample contacts and valleys oriented along major orthogonal directions of our Si(111) samples.

is occupied. As B increases, the six-fold valley degeneracy breaks. Below $\nu = 8$ all integer filling factors have minima, with the even states ($\nu = 6$, 4, and 2) being stronger than the odd ($\nu = 3$, 5 and 7). Below $\nu = 2$, we observe many fractional states with strong minima and associated plateaus at $\nu = 8/5$, $10/7$, and $4/3$.

While $R_{xx} \approx R_{yy}$ at $B = 0$, strong anisotropy appears for $B > 0$. Such anisotropy is to be expected in Si(111) when valleys with different mass tensors have an unequal density of states (DOS) at E_F. If only a single valley is being occupied, and scattering is isotropic, then the theory of Ando [19] predicts that for $m_x > m_y$, $\rho_{xx}/\rho_{yy} = m_x/m_y$, where m_x and m_y are the principal masses of the valley, and the symmetry axes of the resistivity tensor are those of the valley. Using notation appropriate for our system, the model predicts a resistivity anisotropy that lies within the range $0.28 < \rho_{xx}/\rho_{yy} < 3.55$ using $m_x = 0.190 m_e$ and $m_y = 0.674 m_e$.

As noted by Simon in the context of anisotropies at $\nu = 9/2$ [20], the *resistance* anisotropy can greatly exceed the *resistivity* anisotropy in van der Pauw geometry measurements if the symmetry axes of the resistivity tensor are aligned with the device edges [21]. This effect will be largest in our samples when the “C” valleys are being occupied (see the inset to Fig. 1b). The largest resistance anisotropies we observe in our data occur in the range $4 < \nu < 6$ where $R_{yy}/R_{xx} \approx 95$. To account for this we assume that the symmetry axes of ρ are those of the “C” valleys and calculate ρ from R using formulas of Versnel for a circular van der Pauw geometry [22]. The calculated minimum ratio $\rho_{xx}/\rho_{yy} = 0.23$ (see Figure 1b) agrees well with the Ando result when a single “C” valley is being occupied. At lower B, the system is well described by isotropic conduction for $6 \leq \nu \leq 8$, consistent with the approximation that six valleys are being equally occupied in this range. As B is reduced further, however, the anisotropy continues to oscillate due to SdHO. The relative valley occupation is unclear for $2 < \nu < 4$ and therefore we cannot predict the anisotropy.

When $\nu < 2$ we expect that only the final pair of valleys are being occupied and observe a nearly constant resistance anisotropy. The ratio is smaller than that observed at lower B, and the value of R_{xx}/R_{yy} crosses from < 1 to > 1 for $\nu \lesssim 2.25$ ($B \gtrsim 6.7\,\mathrm{T}$). These observations can be explained if either only “A” or “B” valleys are being occupied. Using the equations of Versnel [22], ρ is determined from R assuming that the symmetry axes of ρ are oriented 120° (or equivalently 60°) away from the sample edges. The result, plotted in Fig. 1b again gives a maximum resistivity anisotropy that agrees well with the Ando prediction for a single valley [19]. The anisotropy present in our square samples can therefore be related to the underlying anisotropic mass tensor combined with an unequal valley DOS at E_F.

We focus now on the high B regime of the fractional quantum Hall effect. Figure 2 shows the temperature dependence of R_{xx} in the FQH regime below $\nu = 2$. In this range, we observe 9 states: $\nu = 8/5$, $14/9$, $20/13$, $22/15$, $16/11$, $10/7$, $4/3$, as well as $6/5$ and $14/11$ (not shown). The hierarchy of observed states is exactly that predicted by an SU(2) symmetry in which the two-fold valley degeneracy of electrons is preserved, leading to the creation of composite fermions (CF) with two and four attached vortices (^{2}CF and ^{4}CF, respectively) [23]. From the anisotropy analysis above, the two-fold degeneracy stems from the occupancy of either an “A” or “B” valley pair. For states below $\nu = 1$, the filling factor ν^* of CFs is given by $\nu = \nu^*/(2p\nu^* \pm 1)$ (where $p = 1$ and 2 for ^{2}CF and ^{4}CF, respectively). On the other hand, the hierarchy of fractional states around $\nu = 3/2$, which are the hole-symmetric equivalents to the $\nu = 1/2$ states, is given by $\nu = 2 - \nu^*/(2p\nu^* \pm 1)$ [23]. With an SU(2) symmetry, only $\nu^* = 2, 4, 6, \ldots$ are expected, giving rise to the hierarchy visible in Fig. 2a. A similar, though

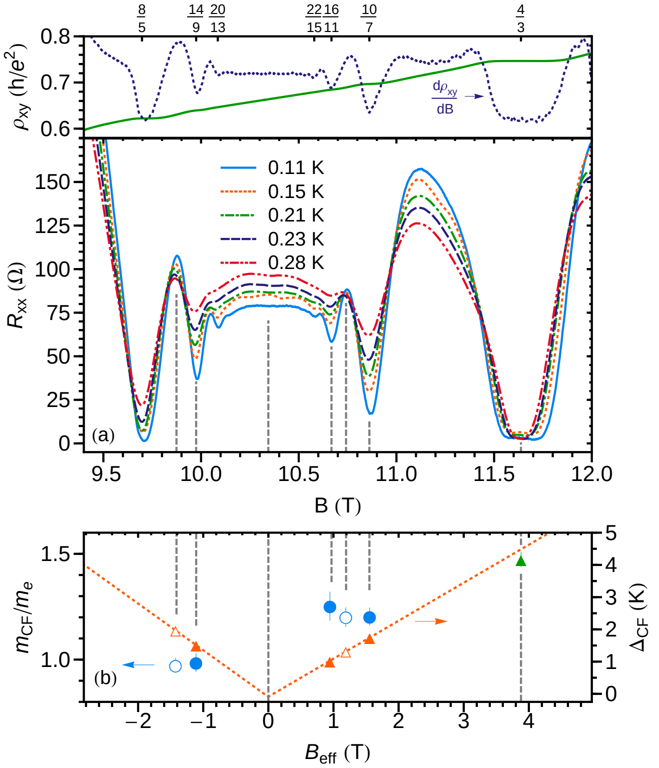

Figure 2. *(a)* R_{xx} vs. B for $n_s = 3.75\times10^{11}\,\mathrm{cm}^{-2}$. Seven FQH states are visible at $T = 110\,\mathrm{mK}$; the filling factors are labeled on the top axis. *Top panel*: ρ_{xy} versus B for $T = 110\,\mathrm{mK}$. The derivative is also shown to accentuate the fine structure, matching the R_{xx} minima. *(b)* Mass of composite fermions assuming that the gaps probed by Shubnikov-de Haas (SdH) oscillations have the form $\Delta_{\mathrm{CF}} = \hbar\omega_{\mathrm{CF}}$. Error bars are the 95% confidence bars from fits to SdH data. On the right axis, the gap energy is plotted for each mass. Open symbols indicate values extracted from maxima. The two lines are fits to available gaps; the intercept for the fits is about $-0.09\,\mathrm{K}$. The gap value at $\nu = 4/3$ is calculated from activation energy data, and is consistent with the extrapolation of the mass.

smaller, hierarchy was observed recently in graphene with the same conclusion [5]. Finally, $\nu = 6/5$ and $14/11$ relate to ^{4}CFs via $\nu^* = 4/3$ and $8/5$, respectively, using $2 - \nu^*/(2\nu^* - 1)$; the ^{4}CF hierarchy simply reflects the FQH states of ^{2}CFs. We note that we observe no evidence for a $\nu = 5/3$ state, similar to recent experiments in both graphene [5] and Si/SiGe [10]. However, the 5/3 state is visible in nominally doubly-degenerate AlAs, probably due to local strains [16, 24, 25].

To estimate the mass of the composite fermions, we use the theory of SdHO and apply it to $\nu = 3/2$ by transforming to an effective magnetic field $B_{\mathrm{eff}} = 3\left(B - B_{3/2}\right)$ where $B_{3/2} = 10.34\,\mathrm{T}$ (calculated from the density) [26]. Although we could use either activation energy measurements or SdHO to find the gaps, analysis based on SdHO takes into account intrinsic level broadening. We first compute the amplitude ΔR of the oscillations using a linear interpolation of the minima and maxima (see [27]). We then use $\Delta R \propto R_0 \exp\left\{-2\pi^2 T_D/\Delta\right\} \xi/\sinh\xi$, where $\xi = 2\pi^2 T/\Delta$, R_0 is the (temperature dependent) resistance at $B_{\mathrm{eff}} = 0$ to find the gap Δ. The Dingle temperature T_D characterizes the intrinsic level broadening.

We expressly assume that $\Delta_{\mathrm{CF}} = \hbar\omega_c^{\mathrm{CF}}$, $\omega_c^{\mathrm{CF}} = e\left|B_{\mathrm{eff}}\right|/m_{\mathrm{CF}}$ and extract m_{CF} directly; the results are shown in Fig. 2b; $m_{\mathrm{CF}}/m_e = 0.98 \pm 0.03$ ($B_{\mathrm{eff}} < 0$), and $m_{\mathrm{CF}}/m_e = 1.20 \pm 0.03$ ($B_{\mathrm{eff}} > 0$). We also plot the gap energy Δ_{CF} as a function of B_{eff}, and fit a line to the resulting energies. The low intercept of $-0.09 \pm 0.07\,\mathrm{K}$ for B_{eff} is consistent with the calculated CF mass. The activation energy at $\nu = 4/3$, measured from higher T data, is consistent with a constant value for m_{CF}. Additionally, we find that all of the FQH data collapses onto a single line for $\Delta R \sinh\xi/R_0\xi$ vs. $1/B$ with $T_D^{\mathrm{CF}} = 180 \pm 8\,\mathrm{mK}$. This is more than twice as large as the value for electrons, where $T_D = 78 \pm 3\,\mathrm{mK}$, determined at low B using the same approach.

While our data is well modeled with a two-fold valley degeneracy, a total-B-dependent valley splitting which polarizes composite fermions, similar to effects due to spin polarization [26], could explain the difference in CF mass between $\pm B_{\mathrm{eff}}$. Such a valley splitting would be consistent with that found in other silicon devices [28, 29]. Additionally, this splitting, which is small and has an upper bound of T_D at $B = 0\,\mathrm{T}$, would also appear in the FQH hierarchy. The derivative in ρ_{xy} in Fig. 2 shows a slight minimum at approximately $\nu = 7/5$, which would be the strongest odd-numerator state for $\nu < 3/2$ for ^{2}CFs. Due to the weakness of the state, however, we conclude that the valley splitting is less than T_D^{CF} at $B_{\mathrm{eff}} = 0$. A significant splitting would also be observed at $\nu > 2$; a weak minimum is seen at $\nu = 7/3$, and is the only odd-numerator state visible. The strength of this state is nonetheless consistent with fractional states due to increasing particle (as opposed to hole) population; measurements on graphene similarly show a hierarchy of the 1/3 family of states [4]. Finally, we note that while our estimates for the CF mass are not entirely consistent with recent measurements on both GaAs [26, 30] and ZnO heterostructures [31], there are several sample-specific effects that could renormalize the CF mass, including the finite perpendicular extent, $z_\perp$, of the electron gas and Landau level mixing [32, 33]. The modification of short-range interactions due to the large dielectric-constant, ϵ, mismatch at the surface is particularly relevant for our devices.

We turn now to gaps at integer filling factors; we use the T dependence of R_{xx} and R_{yy} to calculate the activation energies via $R \propto \exp\left(-\Delta_\nu/2k_BT\right)$. By changing n_s, we are able to measure the gap Δ_ν as a function of B: Figure 3a shows the results of such a calculation in units of the Coulomb energy $E_C = e^2/4\pi\epsilon\epsilon_0 l_B$, where $l_B = \sqrt{\hbar/eB}$ and we use $\epsilon = \left(\epsilon_{\mathrm{Si}} + \epsilon_{\mathrm{Vac}}\right)/2 = 6.25$, which is appropriate for interaction ranges $\gg z_\perp$. Due to

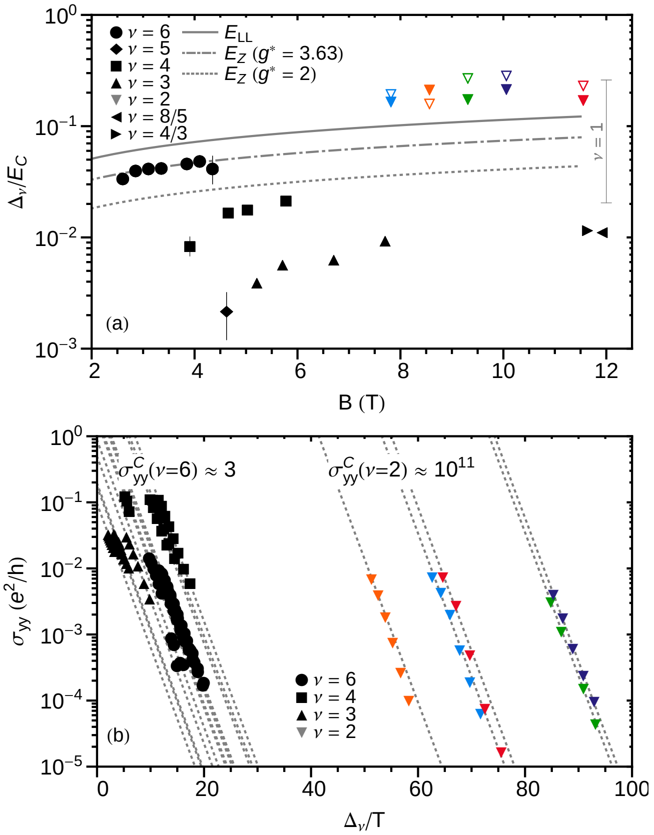

Figure 3. *(a)* Activation energy measurements as a function of B in units of Coulomb energy. Vertical bars show the 95 % confidence errors from fits to the linear portions of Arrhenius plots. Solid symbols indicate data from R_{yy} measurements, while empty symbols are from R_{xx} data. The $\nu = 2$ data shows an enhanced energy gap greater than the Landau level spacing and indicates the scatter between R_{xx} and R_{yy} data. The $\nu = 6$ data is used to extract an effective $g^* = 3.63 \pm 0.06$. *(b)* Plot of the linear portion of σ_{yy} (representative of both directions) versus Δ_ν/T, showing the difference between the critical conductivities σ^C_{yy} at different filling factors and densities. For $\nu = 2$, σ^C_{yy} is between 10 and 16 orders of magnitude larger than the other filling factors (regardless of their density), and the color of each data point is the same in parts (a) and (b).

anisotropy and a lack of large resistance range in R_{xx}, we show only Δ^{yy}_ν for most of the filling factors; for $\nu = 2$ we show both transport directions as an example of scatter in the gap energy.

With the assumption that the valley splitting is smaller than the Zeeman gap, the $\nu = 6$ activation energy is interpreted as $\Delta_6 = E_Z = g^* \mu_B B_{\text{tot}}$, from which we estimate $g^* = 3.63 \pm 0.06$, consistent with previous measurements [17, 18]. The presence of minima at all filling factors $\nu \leq 6$ suggests a B-dependent valley splitting, similar to that observed in SiGe heterostructures [28, 29]. Indeed, the appearance of odd $\nu < 6$ shows that high magnetic fields increasingly break the two-fold degeneracy of opposite $\vec{k}$ valleys. The estimate at $\nu = 5$ is based on a "strength" (S) of the state defined as the ratio of the resistance minimum to the average of the adjacent maxima [10]. From the T dependence, we can estimate a quasi-gap; the state is weaker than any other filling factor $\nu \leq 6$. For $\nu = 1$, we can only estimate an upper and lower bound while noting that the minimum remains visible at $T = 1\,\text{K}$ (see Fig. 3a). The odd filling factor gaps, which are much greater than T_D, indicate that the splitting is likely due to many-body effects.

At $\nu = 2$ one pair of valleys is completely filled, so added electrons must occupy a new valley with a different mass tensor. In this regime, Abanin et al. [16] predict that novel nematic phases are favored, with the sample broken up into domains of differing valley polarization. Experimentally, the temperature dependent behavior at $\nu = 2$ is strikingly different from other filling factors. Indeed, we observe it to be characterized by a very narrow T range where R is thermally activated, leading to a large extrapolated R for $1/T \to 0$ in an Arrhenius plot of the data. In Figure 3b, we show the thermally activated portion of σ_{yy} as a function of Δ_ν/T for the integer filling factors. The critical conductivity $\sigma^C_{yy} = \sigma_{yy}\,(1/T \to 0)$ in the IQH regime is ideally $\sim 2e^2/h$, with reductions possible due to short-range scattering and screening [34–36]. Compared to σ^C_{yy} at higher filling factors, the critical conductivity at $\nu = 2$ is 10 to 16 orders of magnitude larger. Abanin et al. argue that in an anisotropic valley-degenerate system, the transport mechanism in the limit of valley-polarized domains is variable-range hopping due to the low T localization of edge currents along domain walls separating areas of different valley polarization. Fits to different models, including $\sigma = \left(\sigma^{C*}/T\right) \exp\{\Delta_\nu/2k_B T\}$, reproduce the large energy gap and do not reduce the discrepancy in σ^C_{yy} [36]. To the best of our knowledge, the thermal behavior reported here for $\nu = 2$ has not been seen in any other QHE state.

In summary, we have shown evidence of electron-electron interactions in a high mobility Si(111) system. The six-fold valley degeneracy breaks at high magnetic fields into an apparent SU(2) symmetry reflected by the fractional quantum Hall state hierarchy. We estimated the mass of composite fermions near $\nu = 3/2$ by assuming that the Shubnikov-de Haas oscillation gaps can be interpreted as a cyclotron energy. Further experiments are necessary. First, hexagonal samples would allow unambiguous measurements of ρ on Si(111) surfaces. Second, higher magnetic fields are necessary to probe the $\nu < 1$ regime at similar densities, which would shed further light on the valley degeneracy of composite fermions. Finally, tilted magnetic fields would introduce controlled valley splitting of inequivalent valleys [17, 37] and in particular would help shed light on the behavior at $\nu = 2$.

This work was funded by the Laboratory for Physical Sciences. The authors thank Jainendra Jain for useful

discussions.

---

[*] tkott@mailaps.org

[1] D. R. Leadley, R. J. Nicholas, D. K. Maude, A. N. Utjuzh, J. C. Portal, J. J. Harris, and C. T. Foxon, Phys. Rev. Lett. **79**, 4246 (1997).

[2] S. P. Shukla, M. Shayegan, S. R. Parihar, S. A. Lyon, N. R. Cooper, and A. A. Kiselev, Phys. Rev. B **61**, 4469 (2000).

[3] M. Shayegan, E. De Poortere, O. Gunawan, Y. Shkolnikov, E. Tutuc, and K. Vakili, Phys. Status Solidi B (2006).

[4] C. R. Dean, A. F. Young, P. Cadden-Zimansky, L. Wang, H. Ren, K. Watanabe, T. Taniguchi, P. Kim, J. Hone, and K. L. Shepard, Nat. Phys. **7**, 693 (2011).

[5] B. E. Feldman, B. Krauss, J. H. Smet, and A. Yacoby, Science **337**, 1196 (2012).

[6] A. F. Young, C. R. Dean, L. Wang, H. Ren, P. Cadden-Zimansky, K. Watanabe, T. Taniguchi, J. Hone, K. L. Shepard, and P. Kim, Nat. Phys. **8**, 550 (2012).

[7] B. I. Halperin, Helv. Phys. Acta **56**, 75 (1983).

[8] M. Rasolt, F. Perrot, and A. H. MacDonald, Phys. Rev. Lett. **55**, 433 (1985).

[9] M. Rasolt, B. I. Halperin, and D. Vanderbilt, Phys. Rev. Lett. **57**, 126 (1986).

[10] T. M. Lu, W. Pan, D. C. Tsui, C.-H. Lee, and C. W. Liu, Phys. Rev. B **85**, 121307 (2012).

[11] T. B. Boykin, G. Klimeck, M. A. Eriksson, M. Friesen, S. N. Coppersmith, P. von Allmen, F. Oyafuso, and S. Lee, Appl. Phys. Lett. **84**, 115 (2004).

[12] D. C. Tsui and G. Kaminsky, Phys. Rev. Lett. **42**, 595 (1979).

[13] K. Takashina, Y. Ono, A. Fujiwara, Y. Takahashi, and Y. Hirayama, Phys. Rev. Lett. **96**, 236801 (2006).

[14] S. Goswami, K. A. Slinker, M. Friesen, L. M. McGuire, J. L. Truitt, C. Tahan, L. J. Klein, J. O. Chu, P. M. Mooney, D. W. van der Weide, R. Joynt, S. N. Coppersmith, and M. A. Eriksson, Nat. Phys. **3**, 41 (2007).

[15] T. Gokmen, M. Padmanabhan, and M. Shayegan, Nat. Phys. **6**, 621 (2010).

[16] D. A. Abanin, S. A. Parameswaran, S. A. Kivelson, and S. L. Sondhi, Phys. Rev. B **82**, 035428 (2010).

[17] K. Eng, R. McFarland, and B. Kane, Phys. Rev. Lett. **99**, 016801 (2007).

[18] R. N. McFarland, T. M. Kott, L. Sun, K. Eng, and B. E. Kane, Phys. Rev. B **80**, 161310 (2009).

[19] T. Ando, Z. Phys. **24**, 219 (1976).

[20] S. Simon, Phys. Rev. Lett. **83**, 4223 (1999).

[21] M. Lilly, K. Cooper, J. Eisenstein, L. Pfeiffer, and K. West, Phys. Rev. Lett. **82**, 394 (1999).

[22] W. Versnel, J. Appl. Phys. **54**, 916 (1983).

[23] K. Park and J. Jain, Solid State Commun. **119**, 291 (2001).

[24] M. Padmanabhan, T. Gokmen, and M. Shayegan, Phys. Rev. Lett. **104** (2010).

[25] Y. P. Shkolnikov, S. Misra, N. C. Bishop, E. P. De Poortere, and M. Shayegan, Phys. Rev. Lett. **95**, 066809 (2005).

[26] R. Du, A. Yeh, H. Stormer, D. Tsui, L. Pfeiffer, and K. West, Surf. Sci. **361–362**, 26 (1996).

[27] M. Padmanabhan, T. Gokmen, N. C. Bishop, and M. Shayegan, Phys. Rev. Lett. **101**, 026402 (2008).

[28] M. A. Wilde, M. Rhode, C. Heyn, D. Heitmann, D. Grundler, U. Zeitler, F. Schäffler, and R. J. Haug, Phys. Rev. B **72**, 165429 (2005).

[29] P. Weitz, R. Haug, K. von. Klitzing, and F. Schäffler, Surf. Sci. **361-362**, 542 (1996).

[30] W. Pan, H. L. Stormer, D. C. Tsui, L. N. Pfeiffer, K. W. Baldwin, and K. W. West, Phys. Rev. B **61**, R5101 (2000).

[31] D. Maryenko, J. Falson, Y. Kozuka, A. Tsukazaki, M. Onoda, H. Aoki, and M. Kawasaki, Phys. Rev. Lett. **108**, 186803 (2012).

[32] P. J. Gee, F. M. Peeters, J. Singleton, S. Uji, H. Aoki, C. T. B. Foxon, and J. J. Harris, Phys. Rev. B **54**, R14313 (1996).

[33] V. Melik-Alaverdian and N. E. Bonesteel, Phys. Rev. B **52**, R17032 (1995).

[34] N. d'Ambrumenil, B. I. Halperin, and R. H. Morf, Phys. Rev. Lett. **106**, 126804 (2011).

[35] D. G. Polyakov and B. I. Shklovskii, Phys. Rev. Lett. **74**, 150 (1995).

[36] Y. Katayama, D. C. Tsui, and M. Shayegan, Phys. Rev. B **49**, 7400 (1994).

[37] T. Gokmen, M. Padmanabhan, O. Gunawan, Y. P. Shkolnikov, K. Vakili, E. P. De Poortere, and M. Shayegan, Phys. Rev. B **78**, 233306 (2008).